*Proceeding of the Korea Nuclear Society Autumn meeting*
*Seoul, Korea, October 1995*

# Characteristics of Dynamic Strain Aging(DSA) in SA106Gr.C Piping Steel

Jin Weon Kim and In Sup Kim
Korea Advanced Institute of Science and Technology

## Abstract

*Tensile and J-R tests were carried out to estimate the effects of dynamic strain aging(DSA) on SA106Gr.C piping steel. Tensile tests were performed under temperature range RT to 400°C and strain rates from $1.39\times10^{-4}$ to $6.95\times10^{-2}$/s. Fracture toughness was tested in the temperature range RT to 350°C and load-line displacement rates 0.4 and 4mm/min. The effects of DSA on the tensile properties were clearly observed for phenomena such as serrated flow, variation of ultimate and yield stress, and negative strain rate sensitivity. However, the magnitude of serration and strength increase by DSA was relatively small. This may be due to high ratio of Mn to C. In addition, crack initiation resistance, Ji and crack growth resistance, dJ/da were reduced in the range of 200-300°C, where DSA appeared as serrated flow and UTS hardening. The temperature corresponding to minimum fracture resistance was shifted to higher temperature with increasing loading rate.*

## 1. Introduction

Leak-before-break(LBB) concept is now applied to design for high energy piping made by ferritic steel as well as austenitic steel. In the process of LBB analysis, material properties are needed to evaluate leakage-size-crack(LSC) length and crack stability[1]. These material properties have direct influence on the results of evaluation. In particular, for ferritic steel, a decrease of fracture resistance or crack jump, which is believed to be associated with DSA, have been observed in numerous pipe tests and laboratory tests[2]. Therefore, prior to LBB analysis for design it is important to understand the characteristics of DSA in the piping material.

This study carried out the tensile and J-R tests under condition of various strain rates and temperatures to investgate the characteristics of DSA on the SA106Gr.C piping steel.

## 2. Material and Experimental Procedures

The SA106Gr.C carbon steel used in this study was received from Hanjung Co. Ltd., which was archive material of main steam line piping of Young Gwang Units 3 & 4 with dimension of 667mm outer diameter and 28.6mm thickness. The chemical composition is listed in Table1 and the microstructure is a typical ferrite-pearlite structure. Tensile specimens were machined from the midwall location of the pipe such that their tensile axis was parallel with the pipe axis(L-direction). Fracture toughness specimens were in the L-C direction. Tensile specimens

were 48mm gage length and 8mm diameter, and the specimens for fracture toughness test were 1-in thick 10% side-grooved standard C(T) specimens.

The strain rates for tensile test were $1.39\times10^{-4}$, $1.39\times10^{-3}$, $1.39\times10^{-2}$, and $6.95\times10^{-2}$ /s and the range of temperatures was from room temperature(RT) to 400°C. The J-R tests were performed at load-line displacement rates 0.4 and 4mm/min in the temperature range of RT to 350°C. In this study, the direct-current potential drop(DCPD) method was employed to monitor crack initiation and growth. Crack length beyond initiation point for J-R curve was calculated from the post test correction of Johnson's equation[3]. The constant direct-current level was adjusted to give a potential of 200 to 300 μV at the start of test. To prevent a current path through the load train, the specimen was electrically insulated by oxidized zircalloy.

## 3. Results and Discussion

### 1. Characteristics of DSA in SA106Gr.C

From the results of tensile test the serrated flow behaviors, characteristics of dynamic strain aging(DSA)[4], have been observed at certain range of temperatures(Fig.1). The regions where serrated yielding occurred in a certain combination of temperatures and strain rates, are shown in Fig.2. The region of serrated flow was narrow. Also, the magnitude of stress amplitude in serrated flow was relatively small compared with that of the similar plain carbon steels[2]. According to Arrhenius type relation, activation energy for the onset of serration was 29.7kcal/mole, which is larger than activation energies reported from other experimental studies[4,9].

Figs.3 and 4 represent the variation in UTS and yield stress of material with temperature and strain rate. The 0.2% yield stress generally decreased with increase in temperature although there was a plateau at a certain range of temperature. At higher strain rates the plateau was not clear. The yield stresses between RT and 200°C showed the usual positive strain rate dependence. At temperature range of plateau associated with serrated flow, however, positive strain rate dependence of yield stress disappeared and reappeared at 400 °C. As shown in Fig. 4, the UTS of the material varied with temperature, the maxima of UTS occurred around 296 and 375°C and they moved to higher temperatures with increasing strain rate. At RT and 400°C, the UTS increased with increasing strain rate, but the UTS decreased with increasing strain rate at the intermediate temperature, that is negative strain rate sensitivity. Besides serrated yielding in the stress-strain curve, the appearance of UTS peak and negative strain rate dependence of UTS in a particular range of temperature are characteristics of DSA[5].

With increasing temperature, although the elongations showed a scattering as shown in Fig.5, the total elongation decreased gradually to a minimum in temperature range of serrated flow for each strain rate and then increased rapidly, whereas uniform elongation slightly increased or remained in this region of temperature before it decreased.

The behaviors of the tensile properties with temperature and strain rate observed in the present investigation are consistant with present understanding of DSA[5]. However, the magnitude of serration and strength increase by DSA in SA106Gr.C was relatively small in comparison with that in similar carbon steels[2]. In addition, the temperature range of serrated flow was narrow at each strain rate and the temperature range of UTS hardening was higher. These specific characteristics of DSA in SA106Gr.C may be due to higher Mn to C ratio in this material than in the similar carbon steels. Manganese, by forming Mn-C pair, reduces the mobility of the interstitial atoms[6]. With increasing Mn content at constant C content, that is higher value of Mn/C, the interstitial solutes affected by manganese increased in ferrite and the diffusion of interstitial solutes to mobile dislocations in ferrite is relatively slow due to the reduction in mobility of interstitial solutes.

Usually, in a tensile test there is a reduction in both uniform and necking elongation in the DSA region, but in this case reduction in uniform elongation was not observed. This may be due to the continuous work-hardening effect, which is caused by high Mn to C ratio in this material. In the present case, the dislocation locking and resulting interstitial exhaustion may not be high at lower strain region since the diffusion of C to mobile dislocation is more difficult due to presence of Mn. And, the high dislocation multiplication may be limited at initial strain region, while with increasing deformation continuous work-hardening may also occur with DSA. These influences of Mn are supported by higher activation energy at the present investigation.

2. Fracture Resistance of SA106Gr.C

Fig.6 exhibits the J-R curves of material at different temperatures for load line displacement rates of 0.4 and 4mm/min. The effects of temperature and loading rate on the fracture resistance were apparent. To clarify these dependence of material, crack initiation toughness, $J_i$, and crack propagation resistance, $dJ/da$, were obtained from J-R curve. The crack initiation toughness, $J_i$, was defined as value of J-integral at the crack initiation point obtained in the electric potential versus load line displacement curve[7]. As shown in the Fig.7, it was noted that as the temperature increased from ambient, the $J_i$ exhibited lower $J_i$ values until a critical temperature reached and exhibited higher $J_i$ values at higher temperatures. The critical temperatures at which initiation toughness, $J_i$, attained a minimum, were shifted to higher temperature with faster loading rate and were observed at the temperature ranges 200~250°C and 250~296°C for load line displacement rates of 0.4 and 4mm/min, respectively. In these temperature regions, the $J_i$ values decreased by about 30% compared with values at RT for each load line displacement rate. The values of $J_i$ at load line displacement rate of 0.4mm/min were higher than those at 4mm/min at a temperature between RT and 200°C, whereas the values of $J_i$ at 296°C showed negative loading rate dependence. With a further increase in temperature, the dependence of loading rate on $J_i$ became positive again. The variation of $dJ/da$ with temperature for each load line displacement rate is given in Fig.8. These values

have been calculated from linear regression of data points between 0.5 and 2.5mm in physical crack extension(i.e. excluding blunting). As shown in Fig.8, the trend of $dJ/da$ variation with temperatures and loading rates was similar to that of $J_i$ in Fig.7 with exception that the temperatures at which a minimum of $dJ/da$ appeared were higher than those of $J_i$.

As observed in the present study, many investigators have reported the loss of fracture toughness of carbon steel in DSA temperature [8,9,10]. These investigations showed that DSA effect resulted in a decreased fracture resistance of material in the upper shelf region. It is believed that the drop of fracture resistance in DSA region is due to the interaction of the interstitial atoms, such as C and N, with dislocations generated in a well developed plastic zone at the crack front. In the present results, therefore, the temperature difference between minimum points of $J_i$ and $dJ/da$ may be related to the crack tip strain rate. Generally, crack tip strain rate increases with growing the crack[2]. The value of $J_i$ depends on initial crack tip strain rate, whereas $dJ/da$ depends on crack tip strain during crack extension. Thus, DSA effect in the crack growth resistance, $dJ/da$, operates at higher temperature than that in the crack initiation resistance, $J_i$, because of increasing strain rate at crack tip during crack growth.

Typical SEM photographs of the fracture surface obtained after testing at the different temperatures at load line displacement rate of 0.4mm/min are shown in Fig.9. Microscopically, there was an obvious difference in the fracture surface. At RT and 350°C, the large dimples developed at nonmetallic inclusions were seen, while fracture surface at the 200°C consisted of small dimples and cleavages, that is semi-cleavage. This difference of fracture surface is in good agreement with variation of $J_i$ and $dJ/da$ with temperature.

## 4. CONCLUSIONS

1. The effects of dynamic strain aging(DSA) on the tensile properties were clearly observed. However, the magnitude of serration and strength increase by DSA in SA106 Gr.C was relatively small in comparison with that in the plain carbon steel and uniform elongation was not decreased. This may be due to higher Mn/C ratio.
2. $J_i$ and $dJ/da$ in DSA region were about 30~40% lower than those at RT for each loading rate. In addition, the minmum of $J_i$ and dJ/da was shifted to higher temperature with faster loading rate. Thus, the minimum of fracture resistance was observed not at conventional testing condition but rather at other temperatures and loading rates.
3. For material susceptible to DSA, the effects of DSA on the material properties should be considered in the LBB analysis.

## References

1. NUREG-1061, Vol.3, October 1984
2. C.W.Marschall, R. Mohan, P.Krishnaswamy & G.M.Wilkowski, NUREG/CR-6226
3. P.C. McKeigham & D.J.Smith, JTEVA, Vol.22, No.4, p291(1994)
4. A.S.Key, Y. Nakada & W.C.Leslie in "Dislocation Dynamics", McGraw-Hill, 1968

4. A.S.Key, Y. Nakada & W.C.Leslie in "Dislocation Dynamics", McGraw-Hill, 1968
5. J.D.Baird, Met. Rev., Vol.16, p1(1971)
6. C.C.Liand & W.C.Leslie, Metal. Trans.A, Vol.9A, p1765(1978)
7. A. Bakker, ASTM STP 856, p39(1985)
8. M.T.Miglin, ASTM STP 856, p150(1985)
9. S.S.Kang & I.S.Kim, Nuclear Technology, Vol.97, p336(1992)
10. B.Mukherjee, Int. J. Pres. Ves. & Piping, Vol. 31 p363(1988)

Table1 Chemical composition of SA106 Gr.C

| C | Mn | P | S | Si | Ni | Cr | Mo | V | Al | Cu | Hppm |
|---|---|---|---|---|---|---|---|---|---|---|---|
| 0.19 | 1.22 | 0.009 | 0.007 | 0.27 | 0.11 | 0.05 | 0.03 | 0.004 | 0.029 | 0.13 | 1.6 |

c.f) ASME : Mn(max)=1.06 , C(max)=0.35

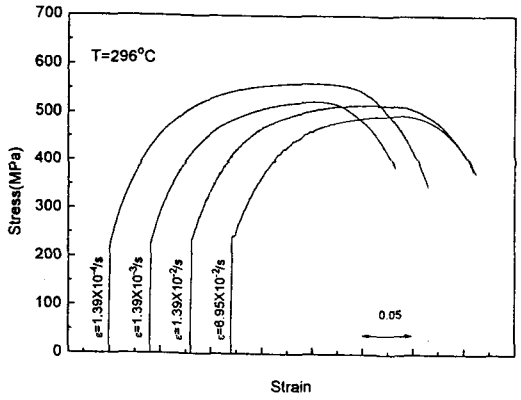


Fig.1 Stress-strain curve with strain rate at 296°C

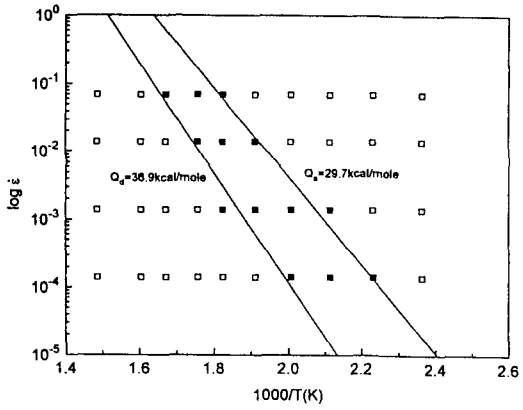


Fig.2 Temperature and strain rate dependence of serrated flow region for SA106Gr.C

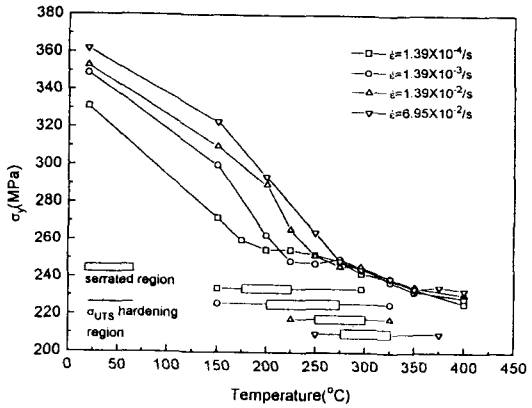


Fig.3 Temperature and strain rate dependence of yield stress

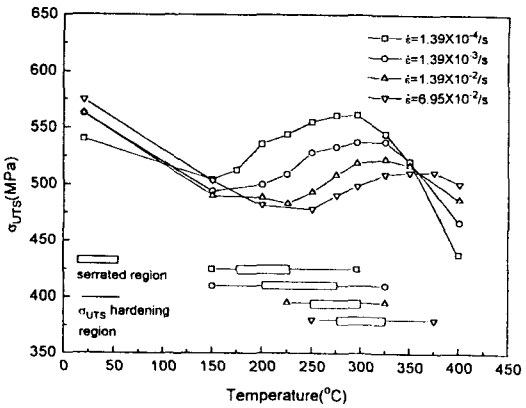


Fig.4 Temperature and strain rate dependence of ultimate tensile stress

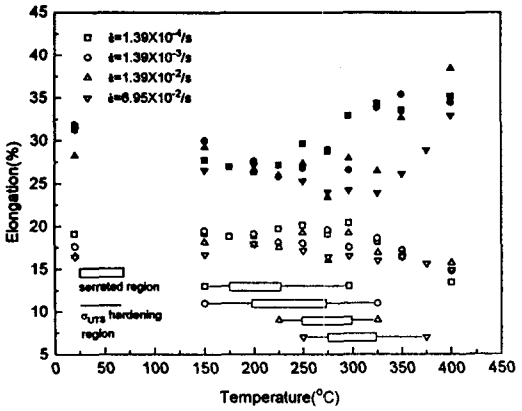


Fig.5 Temperature and strain rate dependence of total and uniform elongation

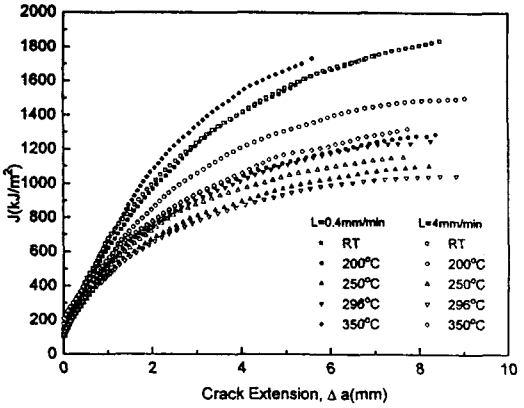


Fig.6 Variation of J-R curve with temperature and load line diplacement rate

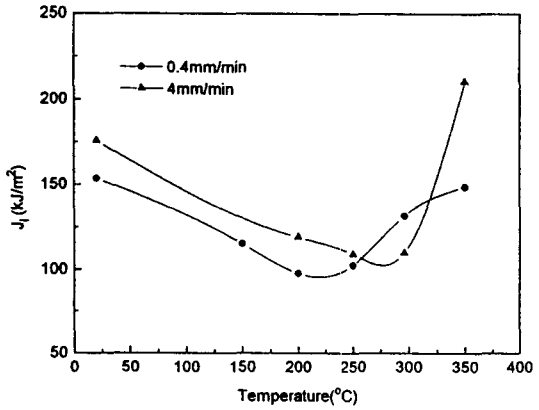


Fig.7 Temperature and strain rate dependence of crack initiation fracture toughness, $J_i$

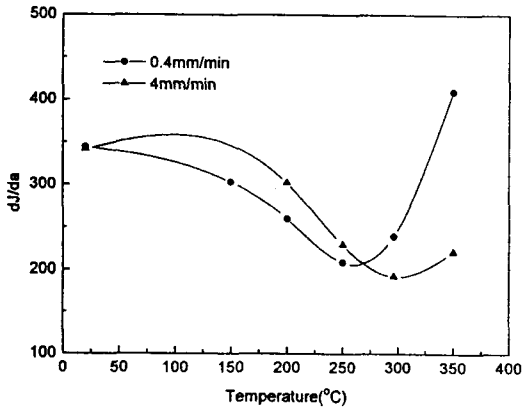


Fig.8 Variation of crack propagation resistance , dJ/da with temperature

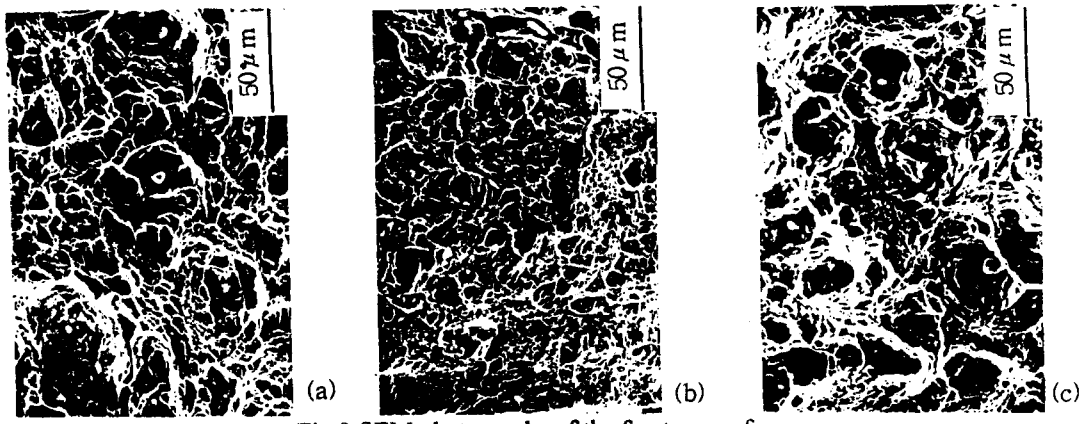


Fig.9 SEM photographs of the fracture surface
(a) RT (b) 200°C (c) 350°C